Progress In Electromagnetics Research C, Vol. 133, 15–25, 2023

5G Indoor Base Station Application: Low Profile Broadband Horizontally Polarized Omnidirectional Antenna

Shihao Wu and Feng Shang*

Abstract—In this paper, a low profile horizontally polarized wideband omnidirectional antenna is presented, which consists of a simple single-layer dielectric substrate planar printing structure. The bottom of the substrate is loaded with six Vivaldi slits to achieve omnidirectional radiation. An equal-amplitude 1 : 6 power-division network is printed on the top of the substrate to provide a uniform feed. In addition, rectangular slots etched on each radiation element conduce to the enhancement of high-frequency gain and improvement of impedance matching. The antenna has 58.8% impedance bandwidth (2.8–5.13 GHz, VSWR < 2) and low profile height of $0.009\lambda_{\min}$, and it is convenient to fix under the ceiling of buildings and could radiate well in indoor place. The radiation mode in the whole operating frequency band is stable, and the cross-polarization is less than -20 dB, which completely covers the 5G NR-n77/78/79 band.

1. INTRODUCTION

Today's mobile communication technology is developing rapidly. The spectrum division is increasingly intensive, and the demand for traffic and data services continues to increase. The high frequency communication gradually takes over the dominant position, which leads to the problem of attenuation and loss. As an important component in communication system, indoor base station antenna can play a role in power compensation to a large extent. Especially in 5G communication, indoor base station antennas with wide band and small size characteristics are indispensable. Omnidirectional antenna is the most common type of indoor communication, which has been widely studied because it can effectively reduce blind area and provide 360° signal coverage. Besides, horizontally polarized (HP) omnidirectional antennas receive higher power indoors than vertically polarized omnidirectional antennas [1]. HP omnidirectional radiation approximates a magnetic dipole (vertical magnetic current), that is, a ring current in the azimuth plane. The electrically small ring antenna is the most direct design method, which has the working mode of magnetic dipole, but the small radiation area leads to poor impedance matching [2]. Although increasing the loop size can improve the impedance, the uneven distribution of loop current makes it impossible to achieve omnidirectional radiation. Alford ring antenna was first proposed in 1940 [3], which better solved this contradiction. Subsequently, modified HP omnidirectional antennas are designed based on the Alford ring structure [4–6], but they have a very narrow bandwidth. In [7], the technology of combining electrically small ring and Alford ring can effectively increase the bandwidth, achieving 4.08% and 14.37% bandwidths, respectively, which is still relatively narrow. In [8], a wider bandwidth of 27.4% was obtained by using a printed coupled ring structure.

Compared with the ring structure, dipole antenna has better design freedom, so it has attracted much attention in the research of omnidirectional antenna. In [9], three broadband dipole elements

Received 24 February 2023, Accepted 10 April 2023, Scheduled 16 May 2023

* Corresponding author: Feng Shang (shangfeng@xupt.edu.cn).

The authors are with the Provincial Key Laboratory of Electromagnetic Field and Microwave Technology, Xi'an University of Posts and Telecommunications, 710121, China.

constitute an array to achieve HP omnidirectional radiation, but the few elements will cause discontinuity of the electric field surface and lead to poor omnidirectional property. For this reason, [10] adopts twelve dipole units for design, which requires a 1 : 12 power division feed network, thus increasing the design complexity. In order to achieve a wide band in a simple structure, in [11, 12] parasitic elements are loaded around the ring dipole, but they have the disadvantages of low gain and large cross-polarization at high frequencies respectively. Thereafter, [13] and [14] enhance the horizontal gain by loading I-shaped structure (ISS) and placing epsilon-negative metamaterial above the antenna, respectively, but the bandwidth of both is narrow. Some novel designs of horizontally polarized antennas [15, 16] are also proposed in the subsequent reports, but they all have the disadvantage of high profile. In [17], a slotted rectangular patch and defective ground are used to realize HP radiation, and the antenna profile is greatly reduced. However, due to its narrow band, it could not be well applied in the design of base station antenna.

Recently, the design method of broadband HP omnidirectional antennas using slit array has been studied [18–20]. In this communication, Vivaldi array is used as the basic structure to design a wideband low profile HP omnidirectional antenna that can be applied to 5G indoor communication. In the following part, the working principle and design process of the proposed antenna are introduced in detail. Finally, a prototype antenna is made, and its performance is demonstrated.

2. BASIC MECHANISM

Tapered slot antenna (or Vivaldi antenna) was first proposed by Gibson in 1979 [21]. It is a kind of traveling wave slot antenna with an exponential conical profile. It has been widely studied because of its characteristics of easy integration in plane and wide band.

A common Vivaldi antenna consists of microstrip feeders, tapered slots, and transition structures. The feeder is often placed across a trough line on the ground. The trough line connects the feeder and tapered slot to play a transitional role, and the electric field energy is radiated through the tapered slot. The antenna as a whole can be identified as a nonuniform conical transmission line [22]. Figure 1 shows

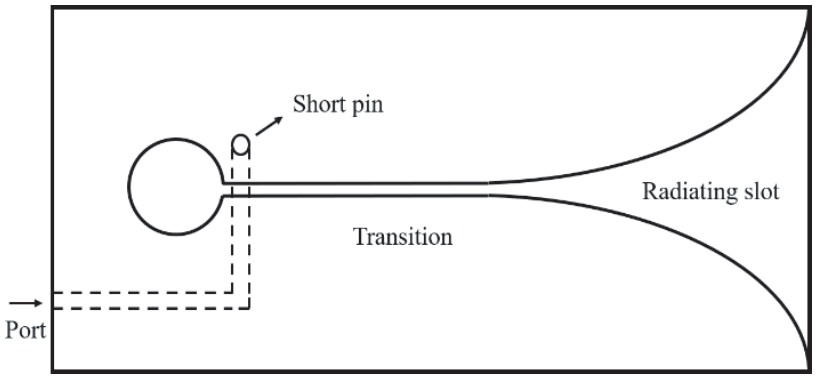

Figure 1. Geometric structure of Vivaldi antenna unit.

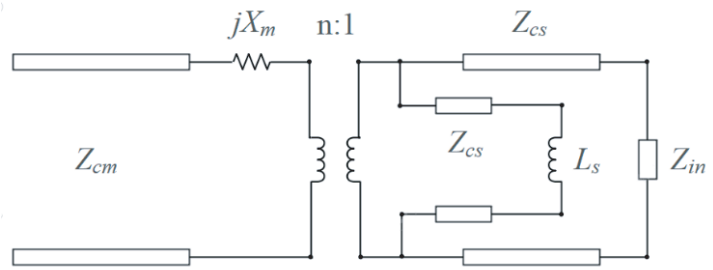

Figure 2. The equivalent circuit model of Vivaldi antenna unit.

the structure diagram of the Vivaldi antenna unit, and its equivalent circuit model is given in Figure 2.

According to the description in [23], Z_{cm} and Z_{cs} represent the characteristic impedance of microstrip feeders and slot lines; L_s is the inductance at the slot end; X_m^{in} and X_s^{in} are the stub reactance of feeders and slot lines; the equivalent inductance introduced by short pin is represented by jX_m; and Z_{in} is the input impedance of microstrip and slot lines. For the convenience of analysis, assume that $Z_{in} = Z_{cs}$, then the input reflection coefficient of the antenna can be obtained:

$$\Gamma_{in} = \frac{R_s - Z_{cm} + j\left(X_m^{in} + X_s\right)}{R_s + Z_{cm} + j\left(X_m^{in} + X_s\right)} \tag{1}$$

where R_s and X_s can be expressed as:

$$R_s = \frac{n^2 X_s^{in} Z_{in}}{Z_{in}^2 + X_s^{in}} \tag{2}$$

$$X_s = \frac{n X_s^{in} Z_{in}}{Z_{in}^2 + X_s^{in}} \tag{3}$$

It can be seen from the above formula that X_m^{in} and X_s are the main factors affecting the input reflection coefficient. This means that the wide band characteristics can be achieved if the feed structure and slot size are properly selected.

In addition, [24] points out that the high dielectric substrate will scatter the surface waves propagating along the antenna, resulting in spurious radiation effect. In contrast, the use of a substrate with low dielectric can effectively reduce the dielectric discontinuity at the end of the Vivaldi antenna and maximize the radiation of the antenna [25]. In the following part, the specific structure and design process of the proposed antenna will be introduced in detail.

3. ANTENNA CONFIGURATION

The structure diagram of the proposed antenna is shown in Figure 3, in which circular F4BME is used as the dielectric substrate with a thickness of 1 mm and a dielectric constant of 2.2. Six Vivaldi arrays loaded with rectangular slots are printed on the bottom of the substrate as radiators, with each cell radiating in the direction of the opening at the edge. A 1 : 6 power-split feed network is printed on the top of the substrate to excite the radiation element, and the feed point is located at the geometric center of the antenna. Detailed parameter dimensions are listed in Table 1.

Table 1. Parameters of the proposed antenna.

Parameter	Value(mm)	Parameter	Value (mm)	Parameter	Value (mm)
$R1$	1.5	$R2$	2.4	$W1$	14.5
$W2$	0.3	A	8 deg	pt	4.9
R_S	1.8	GW	86	$L1$	9.9
$L2$	26.1	$L3$	11	k	0.9
S	0.6				

The exponential tapered profile of the Vivaldi unit is determined by the radian r and the two points A (x_1, y_1) and B (x_2, y_2) at the front and the rear, which allows a large degree of design freedom. The function expression of tapered curve can be obtained by equation as follows [26]:

$$y = C_1 e^{rx} + C_2 \tag{4}$$

$$C_1 = \frac{y_2 - y_1}{e^{rx_2} - e^{rx_1}} \tag{5}$$

$$C_2 = \frac{y_1 e^{rx_2} - y_2 e^{rx_1}}{e^{rx_2} - e^{rx_1}} \tag{6}$$

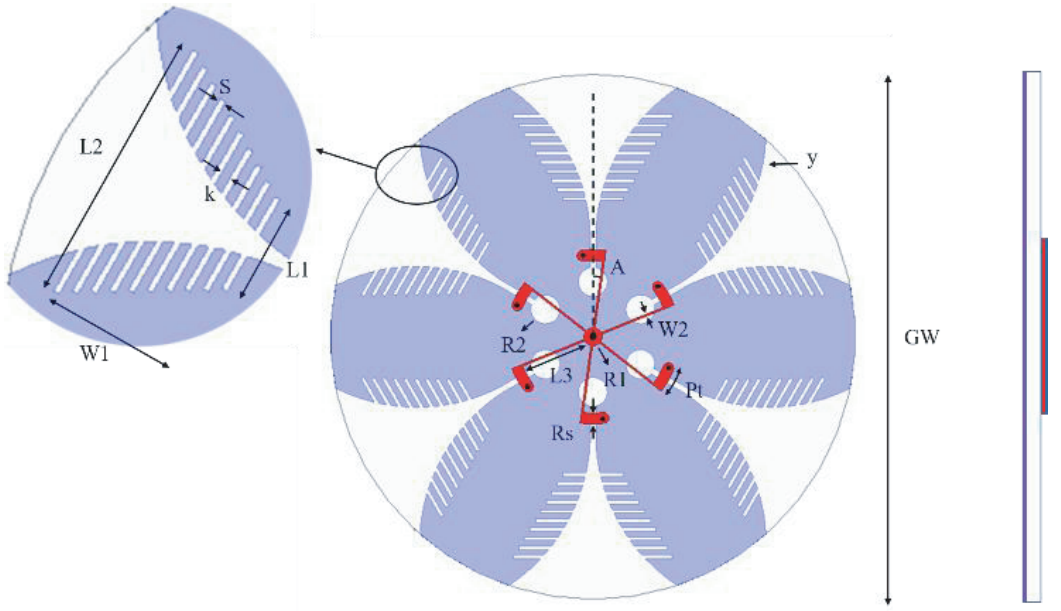

Figure 3. The overall structure of the proposed HP antenna.

where r is the opening rate or radian of the tapered curve. After determining the radian of the slit, C_1 and C_2 can be calculated using the coordinates of the starting point and ending point. The values of these two parameters will directly affect the electrical size of the Vivaldi antenna unit. In this design, the radian $r = 0.1$ then the corresponding $C_1 = 0.25$ and $C_2 = -0.92$.

The left side of Figure 4 shows the schematic diagram of the $1:6$ power distribution feed network of the antenna. A $50\,\Omega$ coaxial cable is fed at the center of the circular patch as the input port, and the fan-shaped balun is connected to the input end of the antenna through a matching transmission line. The feed network in this design has equal amplitude and is in phase, so the structure of each branch is exactly the same, which can be obtained by rotation copy. In order to facilitate design analysis, the equivalent circuit under one of the branches is given on the right side of Figure 4. Considering that the coaxial line of $50\,\Omega$ is connected by six branch microstrip lines in parallel, the input impedance $Z_{in} = 300\,\Omega$. The impedance Z_b of the designed fan-shaped balun is $68\,\Omega$, so the impedance of the matching transmission line can be calculated as $Z_m = \sqrt{Z_{in} \times Z_b} \approx 143\,\Omega$ according to the impedance transformation formula, and the length of the transmission line is about $\lambda_g/4$.

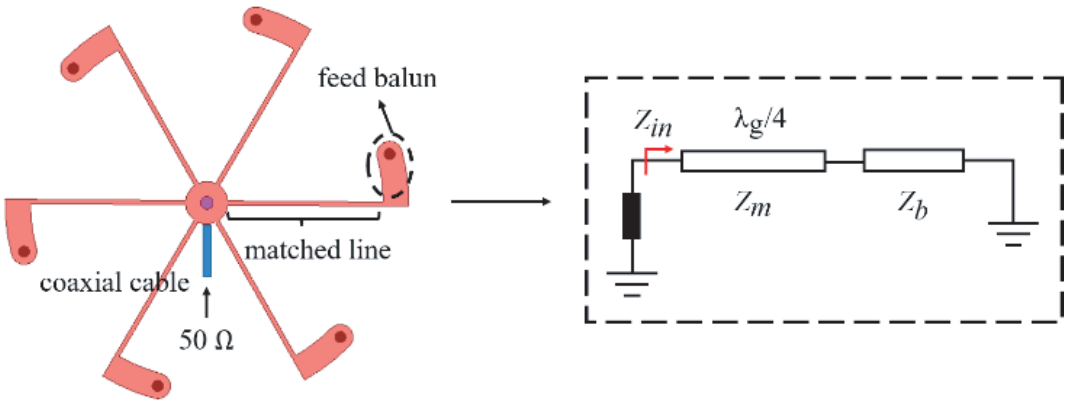

Figure 4. Power division feed network diagram and equivalent circuit.

4. EVOLUTION OF ANTENNA

In order to better analyze the influence of antenna structure on performance, several antenna models in the design process are given in Figure 5. Ant. 1 is the original structure, and the radiation unit consists of only four Vivaldi arrays, which are excited by a 1 : 4 power division network. Ant. 2 increases the number of radiation slits in the original structure to six, which are accordingly excited by a 1 : 6 power splitter. Then, based on Ant. 2, corrugated rectangular slots are introduced on both sides of each radiation slit to form the proposed antenna.

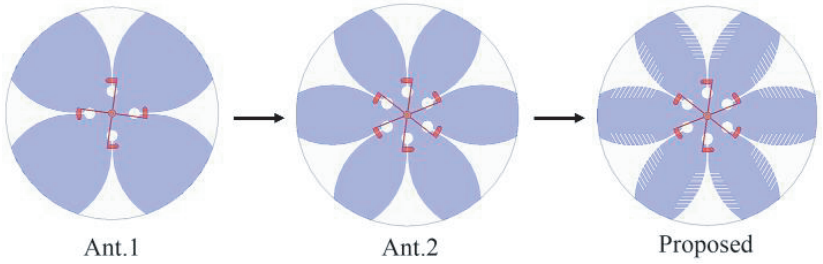

Figure 5. The design evolution of the proposed antenna.

Firstly, the 3D radiation patterns of Ant. 1 and Ant. 2 operating at 3.3 GHz, 4 GHz, and 4.8 GHz are compared, as shown in Figure 6(a) and Figure 6(b). Ant. 1 has a good omnidirectional mode at the low frequency of 3.3 GHz, but the omnidirectional characteristic deteriorates gradually with the increase of frequency. At 4 GHz, the radiation pattern shows a significant ripple in the azimuth plane. When operating at 4.8 GHz, the radiation mode appears to split and distort.

Compared with Ant. 1, Ant. 2 shows stable radiation mode and excellent omnidirectional property at medium and low frequencies. Only slight ripple occurs at 4.8 GHz at high frequencies, but it can remain in omnidirectional mode. It is not difficult to know that the more the number of radiation slits

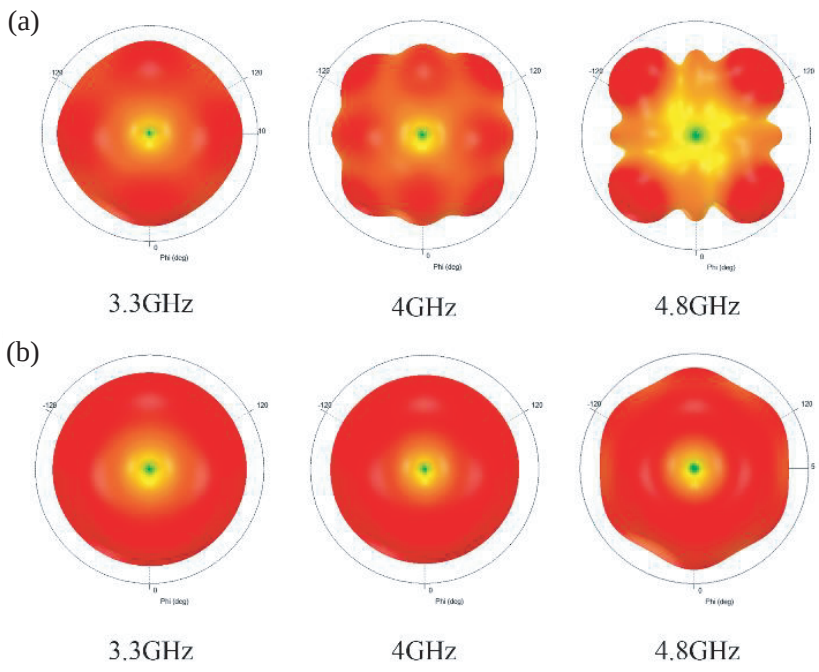

Figure 6. The radiation patterns of Ant. 1 and Ant. 2 at 3.3 GHz, 4 GHz and 4.8 GHz respectively. (a) Ant. 1 with four radiation slits. (b) Ant. 2 with six radiation slits.

is, the better the omnidirectional performance of the antenna is, but it will also complicate the feeding structure, which is disadvantageous to the physical manufacturing. Therefore, in order to balance this point, six radiation slits were selected for design.

By observing the input impedance in Figure 7, it is found that the radiation resistance of Ant. 2 at high frequency is small, while the reactance value is large, so the impedance matching is not good. In order to improve the impedance characteristics, a corrugated rectangular slot structure is loaded. On the one hand, it plays the role of inductive reactance. It can be seen that the resistance value of the proposed antenna at high frequency increases and approaches 50 ohms, and at the same time, the imaginary part of the impedance is close to 0, which means that the impedance matching of the antenna at high frequency is improved.

On the other hand, as shown in Figure 8, the current at the edge of the patch flows along the rectangular slot, extending the current path and increasing the electric length, which is beneficial for maintaining the miniaturization of the antenna.

Moreover, the rectangular slot structure can further enhance the radiation performance of the antenna. Figure 9 compares the realized gains of the antenna before and after loading the rectangular

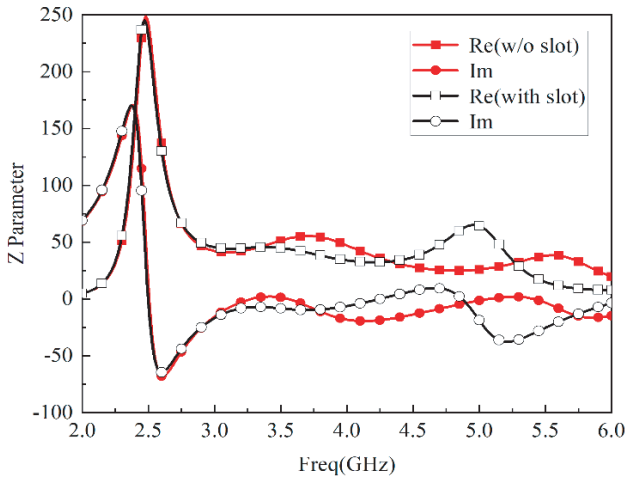

Figure 7. The influence of corrugated rectangular slot on input impedance.

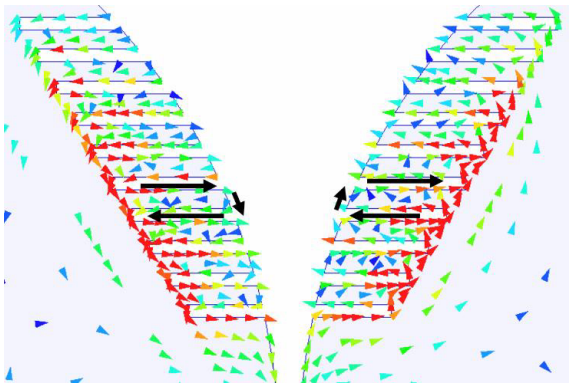

Figure 8. Vector current distribution on both sides of a rectangular corrugated slot.

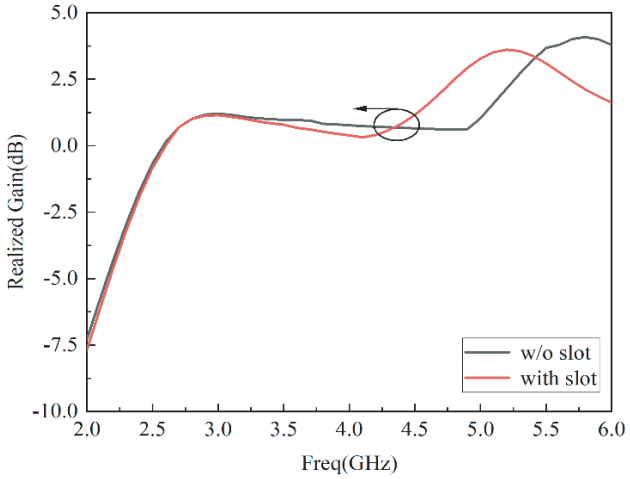

Figure 9. Realized gain curves with and without loaded corrugated slots.

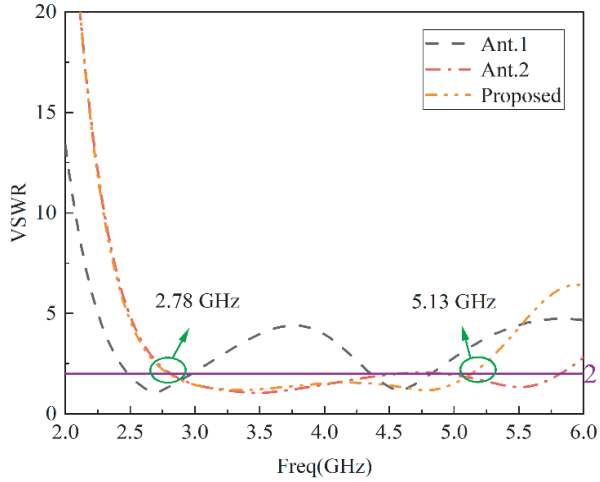

Figure 10. Comparison of VSWR in Ant. 1, Ant. 2 and proposed.

slot. At mid and low frequencies, the realized gain flattens out, while at 4.3 GHz, it starts to show a clear upward trend, and the average gain of the proposed antenna is enhanced by about 1.2 dB in the high frequency band compared to Ant. 2.

Figure 10 shows the comparison of the voltage standing wave ratios (VSWRs) of these three antenna models. Except for the structural changes, the other parameters remain the same. It can be found that Ant. 1 has the narrowest impedance bandwidth, and the resonant points are at 2.7 GHz and 4.6 GHz. In Ant. 2, the impedance bandwidth is significantly broadened, especially between 2.98 GHz and 4.36 GHz.

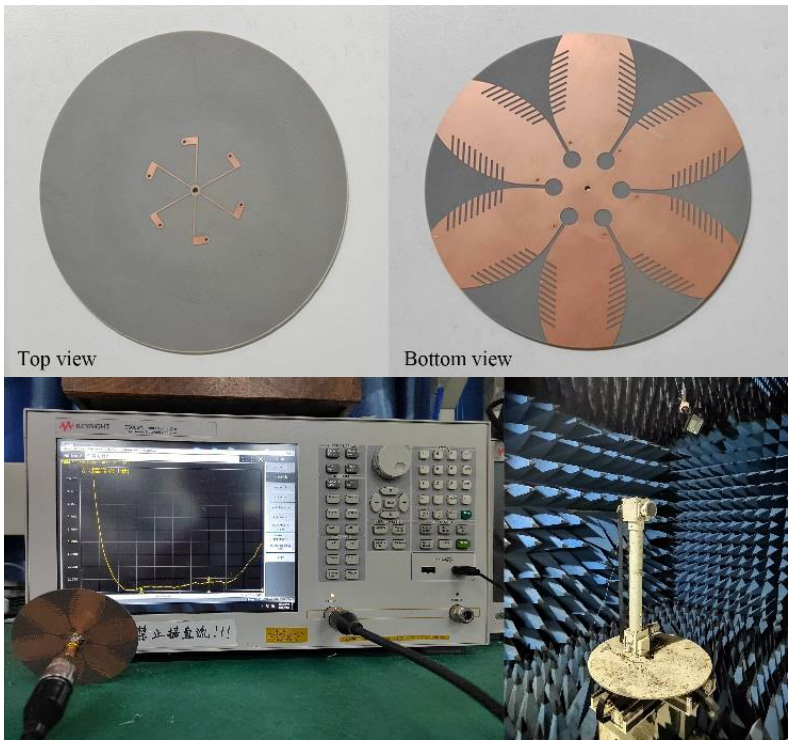

Figure 11. The prototype of the antenna and the measurement scene in the vector network analyzer and microwave anechoic chamber.

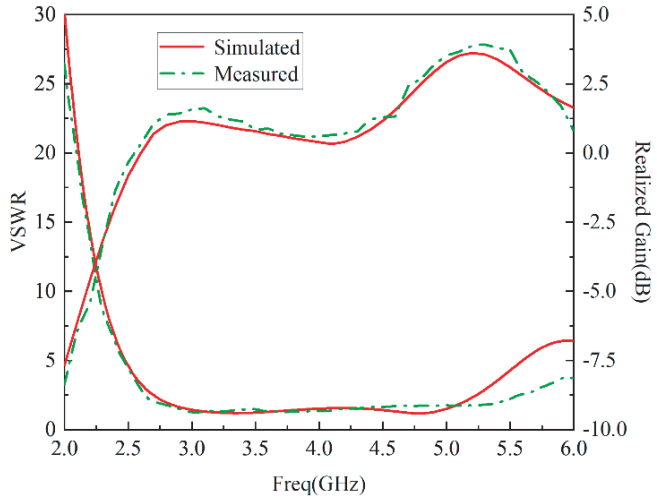

Figure 12. Comparison of simulation and measurement results of VSWR and realized gain.

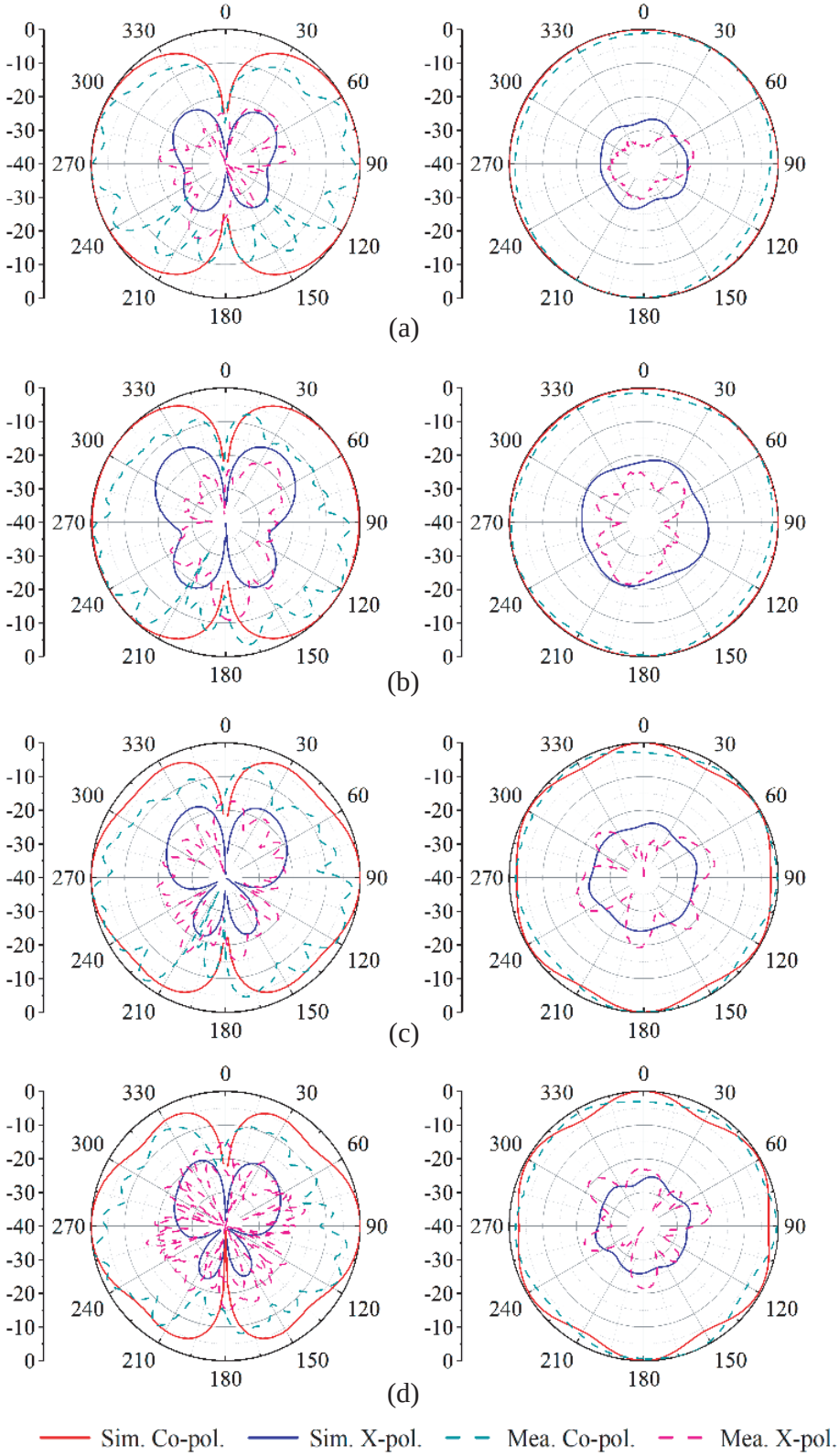

Figure 13. Simulation and measurement of radiation patterns of the proposed antenna. (a) 3.3 GHz. (b) 4 GHz. (c) 4.8 GHz. (d) 5 GHz.

In addition, the resonant frequency moves to high frequency, which is caused by the reduction of the overall size of the antenna radiation patch due to the introduction of multiple radiation slits. In order to further expand the bandwidth at high frequencies, the proposed antenna is loaded with a corrugated structure composed of rectangular slots to achieve a wide impedance bandwidth of 59.6% with VSWR < 2.

5. SIMULATION AND EXPERIMENTAL RESULTS

In order to further verify the design, a prototype antenna was fabricated, and measurements were carried out. Figure 11 shows the actual model and test scenario of the proposed antenna. E5063A vector network analyzer was used to test the voltage standing wave coefficient, and the antenna gain and far-field radiation pattern were measured in a microwave anechoic chamber. Figure 12 depicts the measurement results of voltage standing wave coefficient and gain. Compared with the simulation results, they are basically consistent.

The measured impedance bandwidth is 58.8% (2.8–5.13 GHz), and the peak gain varies between 0.6 and 3.7 dBi.

Figure 13 shows the radiation pattern of the proposed antenna operating at 3.3 GHz, 4 GHz, 4.8 GHz, and 5 GHz, respectively, with stable radiation patterns. Omnidirectional coverage is achieved in the horizontal plane, with slight ripple at the higher frequency, which is caused by the uneven radiation power due to the gain increase. If the antenna is regarded as six planar horn radiating elements, then in the case of the same size, the gain will increase, and the beam will be narrower as the frequency increases, resulting in a decrease in coverage roundness. However, in the overall direction, the minimum gain is also greater than -0.43 dBi, and the omnidirectional radiation can be well carried out. The maximum unroundness is about 4.5 dB. At the same time, the cross polarizations of horizontal plane and vertical plane are less than -20 dB and -15 dB. In addition, Table 2 also lists the comparison between some previous research works and the design of this paper.

Table 2. Comparison of the proposed antenna with the reference antennas.

Ref.	Bandwidth (%)	Gain (dBi)	Dimension ($\lambda^3_{\min}$)
[8]	27.4	1.4	$0.50 \times 0.50 \times 0.02$
[13]	19	1.8	$0.77 \times 0.77 \times 0.05$
[14]	9.3	2.99	$1.85 \times 1.85 \times 0.08$
[15]	18.1	0.98–2.04	$0.48 \times 0.48 \times 0.19$
[16]	5.32/20.56	≈ 2	$0.18 \times 0.08 \times 0.20$
[17]	5.51	2.3	$0.32 \times 0.32 \times 0.006$
Prop.	58.8%	0.6–3.7	$0.80 \times 0.80 \times 0.009$

6. CONCLUSION

In this paper, a wideband HP omnidirectional antenna is proposed to achieve an omnidirectional radiation pattern by forming an array of six Vivaldi slit elements as radiators. A simple $1:6$ power division network is used for feeding. All structures are printed on the front and back sides of a single dielectric substrate, giving it the advantage of a low profile, while also helping to reduce design costs and have ease of fabrication. The proposed antenna has a VSWR < 2 in the 2.78–5.13 GHz range and achieves 58.8% broadband characteristics. It can fully cover 5G NR-n77/78/79 frequency band, which can be used as a candidate for 5G indoor micro-base station.

REFERENCES

1. Wei, K., Z. Zhang, and Z. Feng, "Design of a wideband horizontally polarized omnidirectional printed loop antenna," *IEEE Antennas Wireless Propag. Lett.*, Vol. 11, 49–52, 2012.
2. Park, J.-S. and H.-K. Choi, "The design of broadband omnidirectional horizontally polarized dipole antennas with branch lines," *Microw. Opt. Technol. Lett.*, Vol. 57, 2901–2905, 2015.
3. Alford, A. and A. G. Kandoian, "Ultrahigh-frequency loop antennas," *Electrical Engineering*, Vol. 59, No. 12, 843–848, Dec. 1940.
4. Lin, C.-C., L.-C. Kuo, and H.-R. Chuang, "A horizontally polarized omnidirectional printed antenna for WLAN applications," *IEEE Trans. Antennas Propag.*, Vol. 54, No. 11, 3551–3556, Nov. 2006.
5. Ahn, C.-H., S.-W. Oh, and K. Chang, "A dual-frequency omnidirectional antenna for polarization diversity of MIMO and wireless communication applications," *IEEE Antennas Wireless Propag. Lett.*, Vol. 8, 966–969, 2009.
6. Park, J.-S., H.-K. Choi, and J.-H. Oh, "The design of a dual band omnidirectional horizontally polarized antenna with arc-shaped lines and overlapping lines," *Microw. Opt. Technol. Lett.*, Vol. 58, 1117–1121, 2016.
7. Hu, P. F., K. W. Leung, Y. M. Pan, and S. Y. Zheng, "Electrically small, planar, horizontally polarized dual-band omnidirectional antenna and its application in a MIMO system," *IEEE Trans. Antennas Propag.*, Vol. 69, No. 9, 5345–5355, Sept. 2021.
8. Li, X. D., Y. H. Ren, H. D. Wu, F. Cui, K. Li, and F. W. Wang, "A low profile wideband horizontally polarized omnidirectional printed loop antenna," *Int. J. RF Microw. Comput.-Aided Eng.*, Vol. 32, No. 2, Art. No. e22980, Nov. 2021.
9. Ye, L. H., Y. Zhang, X. Y. Zhang, and Q. Xue, "Broadband horizontally polarized omnidirectional antenna array for base-station applications," *IEEE Trans. Antennas Propag.*, Vol. 67, No. 4, 2792–2797, Apr. 2019.
10. Wang, Z. D., Y. Z. Yin, X. Yang, and J. J. Wu, "Design of a wideband horizontally polarized omnidirectional antenna with mutual coupling method," *IEEE Trans. Antennas Propag.*, Vol. 63, No. 7, 3311–3316, Jul. 2015.
11. Zhu, Q., S. Yang, and Z. Chen, "A wideband horizontally polarized omnidirectional antenna for LTE indoor base stations," *Microw. Opt. Technol. Lett.*, Vol. 57, 2112–2116, 2015.
12. Yu, Y., F. Jolani, and Z. Chen, "A wideband omnidirectional horizontally polarized antenna for 4G LTE applications," *IEEE Antennas Wireless Propag. Lett.*, Vol. 12, 686–689, 2013.
13. Liu, A. K., L. Huang, and Y. Lu, "Wideband circular patch antenna with I-shaped structure for horizontal omnidirectional gain enhancement," *IET Microw., Antennas Propag.*, Vol. 13, No. 5, 608–614, Apr. 2019.
14. Guo, Y., J. Zhao, Q. Hou, and X. Zhao, "Omnidirectional broadband patch antenna with horizontal gain enhanced by epsilon-negative metamaterial superstrate," *Microw. Opt. Technol. Lett.*, Vol. 62, No. 2, 778–788, Oct. 2019.
15. Liu, X., K. W. Leung, and N. Yang, "Wideband horizontally polarized omnidirectional cylindrical dielectric resonator antenna for polarization reconfigurable design," *IEEE Trans. Antennas Propag.*, Vol. 69, No. 11, 7333–7342, Nov. 2021.
16. Guo, J., H. Bai, A. Feng, Y. Liu, Y. Huang, and X. Zhang, "A compact dual-band slot antenna with horizontally polarized omnidirectional radiation," *IEEE Antennas Wireless Propag. Lett.*, Vol. 20, No. 7, 1234–1238, Jul. 2021.
17. Santra, G. and P. N. Patel, "Horizontally polarised omnidirectional antenna using slotted rectangular patch and defected ground structure," *IEEE Antennas Wireless Propag. Lett.*, 1–5, Nov. 2022.
18. Liu, H., Y. Liu, W. Zhang, and S. Gao, "An ultra-wideband horizontally polarized omnidirectional circular connected Vivaldi antenna array," *IEEE Trans. Antennas Propag.*, Vol. 65, No. 8, 4351–4356, Aug. 2017.

19. Jiang, G. and C. Guo, "A broadband horizontally polarized omnidirectional antenna array consisting of four corrugated TSA elements," *2016 CIE International Conference on Radar (RADAR)*, 1–5, 2016.
20. Lei, Z., C. Mantang, and L. Yangyi, "A broadband horizontally polarised omnidirectional antenna with stable radiation patterns," *The Journal of Engineering*, Vol. 19, 5722–5725, 2019.
21. Gibson, P. J., "The Vivaldi aerial," *1979 9th European Microwave Conference*, 101–105, Brighton, UK, 1979, doi:10.1109/EUMA.1979.332681.
22. Janaswamy, R. and D. Schaubert, "Analysis of the tapered slot antenna," *IEEE Trans. Antennas Propag.*, Vol. 35, No. 9, 1058–1065, Sept. 1987.
23. Deng, C. and Y.-J. Xie, "Design of resistive loading Vivaldi antenna," *IEEE Antennas Wireless Propag. Lett.*, Vol. 8, 240–243, 2009.
24. Burrell, D. A. and J. T. Aberle, "Characterization of Vivaldi antennas utilizing a microstrip-to-slotline transition," *Proceedings of IEEE Antennas and Propagation Society International Symposium*, Vol. 3, 1212–1215, 1993.
25. Mirshekar-Syahkal, D. and H. Y. Wang, "Single and coupled modified V-shaped tapered slot antennas," *IEEE Antennas and Propagation Society International Symposium*, Vol. 4, 2324–2327, 1998.
26. Balanis, C. A., *Antenna Theory: Analysis and Design*, 2nd Edition, Wiley, New York, 1997.